



Improving the Microstructure and Mechanical Properties of Aluminium Alloys Joints by Adding SiC Particles During Friction Stir Welding Process

Mohammed Hadi Ali¹ · Haitham M. Wadallah² · Mohsen Abaid Ibrahim¹ · Omar Rafae Alomar²

Received: 9 January 2021 / Accepted: 7 April 2021 / Published online: 27 May 2021
© ASM International 2021

Abstract

This study experimentally investigates the influence of adding SiC on microstructure and mechanical properties of the aluminium alloys welded joints. The SiC particles have been directly added into a zone of friction stir welding (FSW) to make (AA6061–AA2024) SiC composites material. Results show that the effect of adding SiC particles on microstructure refines the grain size in the stir zone by preventing its growth during FSW process. The adding of SiC particles has a significant effect on the thermomechanical zone resulting from restricting the growth of grains. Results indicated that the microhardness of FSW joints is increased from 44 to 86 HV by adding 9.2% SiC particles as compared to that obtained without including SiC under the same welding conditions. It has been observed that the tensile strength is enhanced when the amount of SiC particles are increased by up to 6.9%.

Keywords SiC particles · Aluminium alloys · Metal matrix composites · Scanning electronic microscope · Friction stir welding

Introduction

The topic of metal matrix composites (MMCs) continues to attract interest in several engineering applications due to their specifications. Dinaharan [7] presented an example of MMCs that given a great interest in the last decade, the mechanical properties are improved significantly regardless of the type of reinforcement added. Gangil et al. [11] pointed out that the MMCs can be found in many fields such as automobile and aerospace. Zhang et al. [27] added that aluminium matrix composites are considered as one of the most important types of composites materials. Generally, the properties and the performance of aluminium matrix composites depend on several aspects. For example, Güler and Bağcı [12] reported that the size is of great importance and on the other hand the distribution of the reinforcing particles

affects as well as the interfacial bonding between the reinforcing particles and the matrix. Azimi-Roeeen et al. [4] summarised that friction stir welding (FSW) has been used to produce MMCs, and hence, it is considered relatively a new solid-state welding method. Mishra and Ma [15] reviewed this kind of welding, i.e. FSW has been developed in 1991 by the Institute of The United Kingdom Welding. The FSW is represented as an effective welding process that is used for welding metals via using a special tool, which is complicated to weld it by utilizing the fusion welding method. Prakash et al. [18] have concluded that FSW has many advantages in comparison with the traditional methods, and thus, it has been considered environmentally friendly, economical and defect free. Elatharasan and Kumar [8] also pointed out that FSW can be used in the fabrication of surface composites materials.

Sun and Fujii [22] performed an experimental study to investigate the effect of adding SiC particles with 5 µm mean size to the pure Cu joints through FSW. In their study, the results show that the spreading of SiC is non-uniform and surrounded by pores after one pass. After two passes, on the other hand, the particles became more uniform. The particle at the banded structure became rich (i.e. less than 2 µm size) and free region with approximately 8 µm size at the SZ area.

✉ Omar Rafae Alomar
omar.alomar@ntu.edu.iq; sedrarasha@yahoo.com

¹ AL-Suwaira Technical Institute, Middle Technical University, Baghdad, Iraq

² Engineering Technical College of Mosul, Northern Technical University, Cultural Group Street, Mosul, Iraq

In addition, the results show that the particles of SiC can play as heterogenous nucleation sites in the Cu grains, and dynamic recrystallization occurs. It also leads to a higher hardness value 110 HV joint Vickers hardness as compared to 70 HV in the SZ zone without strengthening by SiC.

Zhao et al. [28] investigated the effect of the FSW process on the mechanical properties and microstructure of nano-ZrB₂/2024 aluminium alloy composite fabricated from the system of 2024Al–K₂ZrF₆–KBF₄ to attain the composite superplasticity. In their study, different reinforcement ratios (1, 3 and 5%), strain rate of (5×10^{-3} , 1×10^{-2} and $2 \times 10^{-2} \text{ s}^{-1}$) and temperature (400, 480, 600, 700 and 750 K) have been used. The results indicated that the FSW redistributes the ZrB₂ agglomerate to uniform particles and refining the matrix grains. Besides, it has been found FSW composites have higher ostensible deformation activation energy than that with pure aluminium. Deepak et al. [6] prepared a composite surface of aluminium alloy 5083 reinforced and nano-SiC by using FSW in order to study their mechanical properties and wear behaviour. In their study, it has been observed that the hardness is increased particularly at the stir zone as compared to aluminium alloy 5083. It is also evident that the based alloy has a lower wear rate as compared to surface composite fabricated by FSW tribological due to the higher friction coefficient and force established during the sliding wear course. Thangarasu et al. [24] fabricated an aluminium surface composite (AA6082/TiC) by employing the FSW process in order to study the impact of speed welding on the mechanical properties while keeping the parameters of groove width, axial force and tool rotational speed constant. The results demonstrate that the speed of welding has a considerable influence on the area of the welding zone. The results also show that the low speed of welding improves the distribution of TiC and more homogeneity and decreases the hardness and increases the wear rate.

Yuvaraj and Aravindan [25] used the FSW process to fabricate an aluminium surface composite (5083/B4C). The size of the reinforcement of nano- and microparticle and the number of passes have been studied. Results show those better mechanical properties and wear resistance have been obtained when using a nanoparticle size of reinforcement with the number of passes equal to three as compared to the base material. Pasha et al. [16] conducted an experimental study to analyse the influence of adding the SiC particles as reinforcement to the magnesium alloy (AZ31B) plate using FSW. The magnesium alloy (AZ31B) plate has been tested under two different conditions, which unreinforced and reinforced welded conditions. In their study, different volume fractions of SiC have been employed at 10, 15, 25 and 30% with 1400 rpm rotational and 25 mm/min transverse speeds. The results indicated that the mechanical properties of SiC–Mg alloy AZ31B welded joints are increased as compared to unreinforced conditions. It has been also

observed that the strength has been increased when the volume fraction of SiC in the ranges of 10–25% and is decreased when the volume fraction is further increased by up to 30%. Rathee et al. [19] fabricated AA6061/SiC composites surface using FSW to study the tool plunge depth effects on the dispersal of strengthening particles. In their study, the 6061 alloy sheet with 5mm thickness, six variable tool plunge depth, constant diameter of shoulder levels, 2.5° tool tilt angle, 1400 rpm rotational speed and 40 mm/min travel speed have been used. The results show that the low depth reduces heat generation during welding which leads to defect in the NZ area such as the cavity. Also, it has been observed that the high plastic strain and stirring action of friction stir paces tool lead to fragmentation of SiC particles.

Acharya et al. [1] investigated the impact of the rotation speed of the tool on the particle distribution of aluminium 6092-17.5 SiCp-T6 composite plate using FSW. In their study, a plate with 6 mm thickness, 2° tool tilt angle with 1 mm/s travel speed and (1000–2000) rpm TRS have been used. The results show that the uniform distribution with maximum joint efficiency has been obtained when the value of welding tool rotation speed is between 1000 and 1500 rpm. Furthermore, it has been found that the distribution of SiC particles at the NZ area is more evident in the transverse direction in comparison with the axial direction. Singh et al. [21] fabricated a nanocomposites material made from Al6061–Al₂O₃ using FSW. In their study, the Al₂O₃ nanoparticles have been added by making cylindrical holes with 1.5 mm (diameter), 3 mm (depth) and the distance between the holes equal to 13.3 mm. It has been observed that the addition of Al₂O₃ nanoparticles increases grain refinement in the NZ area. Furthermore, the adding of Al₂O₃ nanoparticles prevents grain growth and decreases grain size. The results also indicated that the hardness value in the NZ area is increased. Pol et al. [17] fabricated AA7005/B4C and TiB₂ composites surface to evaluate ballistic behaviour by using a variable percentage of B4C and TiB₂. The results show that the B4C and TiB₂ have no effect on hardness due to the reinforcement particle has a similar size. The results also show that the 70 HV hardness for the composite is higher than the base metal and 20–60 mm penetration depth for steel in comparison with 37 mm in the base alloy. The ballistic mass efficiency factor is 1.6 times higher than the base alloy.

A careful look into the literature review related to FSW in the field of metal matrix composites reveals that great attention has been focused and given to the fabrication of surface composites materials for the same alloy. Furthermore, the review of literature also exposes that there are few studies used the FSW for preparing a composite metal by directly adding the particles of SiC in the welding area and most of these studies have been concerned with adding SiC to a surface. Therefore, the present study aims to prepare

Table 1 Chemical composition of AA2024 and AA6061 aluminium alloys

Elements	AA2024	AA6061
Cu	4.5	0.372
Si	0.110	0.752
Mg	1.23	1.08
Fe	0.313	0.599
Cr	0.026	0.239
Mn	0.566	0.090
Zn	0.147	0.071
Ni	0.01	0.008
Ti	0.018	0.009
V	0.008	0.005
Pb	0.015	0.015
Al	Bal	Bal

metal matrix composites for two different aluminium alloys (AA2024 and AA6061) by directly adding SiC particles in the welding area (stir zone) using the FSW process through making a groove between the two pieces and to study the influence of addition particles of SiC on the improvement of the mechanical properties and microstructure of the welding area.

The present paper is constructed as follows. The experimental set-up and the procedure are described in Sect. 2. The results are discussed and presented in Sect. 3. Finally, the conclusions obtained from the present study are drawn in Sect. 4.

Experimentation

The experiments have been conducted by using two different materials of aluminium alloy. These materials are the plates of AA2024 and AA6061 aluminium alloys. These two plates have a thickness of 6, 85 mm in width and 150 mm in length. Table 1 presents the chemical composition of the materials. Silicon carbide powder has been added to the welding area by creating a groove in the welding line between the two pieces. The size of SiC powder that has been used as reinforcement particles equal to 5 μm and other properties are given in Table 2. The SiC powders have been supplied from BDH chemicals Limited, England. During the welding process, the rotation of the welding tool have been selected to be 1040 rpm and the welding speed equal to 30 mm/min, and these parameters have represented the maximum speed of the device used in the experiments. The welding tool has been made from stainless steel (T31501, O1). The shoulder has a diameter equal to 18 mm, whereas the pin has 6 mm and 5.75 mm in length. The FSW process of aluminium alloys with and without adding SiC particles and the joint after welding are displayed in Fig. 1. The dimensions of the

Table 2 Physical properties of SiC particles

Purity, %	Particle size, μm	Density, g/cm^3	Hardness, Mohs
99.9	3–5	3.216	9.5

groove and ratio of reinforcement of SiC are presented in Table 3.

To examine the microstructure of the welding area, optical and scanning electron microscopy has been used to test the base alloy and the welding joints with and without adding the SiC reinforcement. Furthermore, the EDS test has been employed to evaluate the chemical composition of the phases that appeared in the microstructure. The SiC paper with different grits up to 1200 has been utilized for the grinding process, whereas the diamond paste along with lubricant has been used for the polishing process. Then, the samples have been etched by using Keller reagent. Finally, the samples have been washed with water and alcohol and then dried. The hardness test has been performed using the Vickers hardness device, where the load has been used equally to 500 g for 15 s. This test has been conducted every 2 mm along with a cross section of the welding joints. The tensile specimens of FSW, based on ASTM E8, have been prepared for two samples under each condition. The dimensions of tensile specimens with and without adding particles of SiC are shown in Fig. 2. The X-ray test has been also used to define the microstructure phases in the joint area (i.e. stir and thermomechanically affected zones). This test has been done by using the Miniflex II device and Cu targets with 40 KV. Figure 3 shows the X-ray pattern of FSW joints with the reinforcement ratio of SiC equals 4.6%.

Results and Discussion

The major objective of this work is to experimentally examine the effect of directly adding the Sic particles in the welding area during the process of friction stir welding (FSW) to generate metal matrix composites of two different aluminium alloys (AA2024 and AA6061). As a consequence, the experiments have been conducted for various reinforcement ratios of SiC that are presented in Figs. 4, 5, 6, 7, 8, 9, 10 and 11. It would, therefore, be worthwhile to explore the impact of adding SiC particles on the composite material as compared with that obtained without adding SiC particles.

Microstructure

Figure 3 shows the phases that appeared using the X-ray test. These phases are AlCu, Al₃Mg₂, CuAl₂ and Cu₂Al₂ phase in addition to SiC. These phases are a mixture of the phases that appear in both alloys (AA2024 and AA6061).

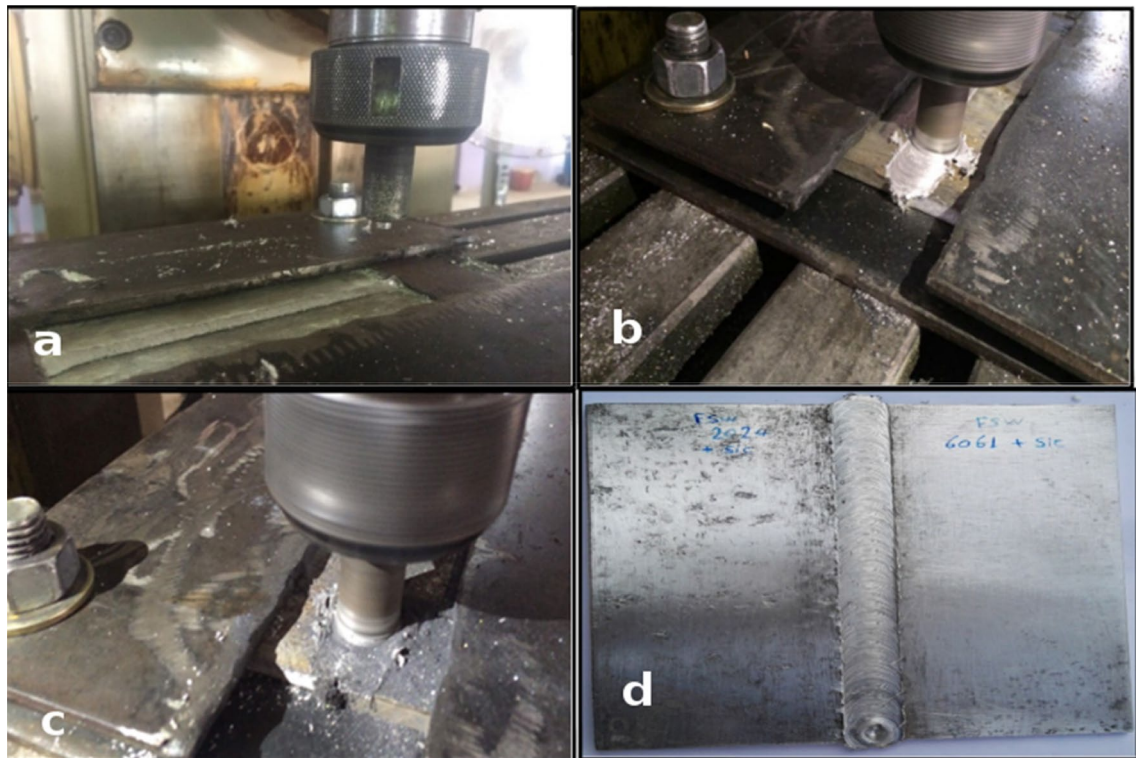


Fig. 1 Process of (a) FSW, (b) welding without adding particles of SiC, (c) welding with adding particles of SiC and (d) joints of AA2024 and AA6061 alloys

Table 3 Dimensions of the groove and ratio of reinforcement of SiC

Cases	Reinforcement of SiC, %	Width of the groove, mm	Depth of the groove, mm
A	4.6	2.5	2
B	6.9	2.5	3
C	9.2	2.5	4

Figure 4a shows the microstructure of the AA2024 alloy, whereas Fig. 4b displays the microstructure of the AA6061 alloy. As a consequence, it is clear from Fig. 4a that the alloy phases have been characterized by coarse size, whereas the alloy phases in Fig. 4b has a somewhat coarse size. The

appearance of Fe element in the results of EDS analysis is related to the original components of the two basic alloys as shown in Table 1 as well as mentioned by [26].

The thermomechanical deformation in the TMAZ area leads to the longitudinal grains having a direction with the deformation line, as shown in Fig. 5a–e. The particles of SiC have been distributed in the deformation lines at the TMAZ area. On the other hand, the SiC particles have a cluster form and it is characterized by a moderate size, where the fine particles are gathered behind the coarse particles of the clusters at the same deformation lines. As shown in Figs. 4b, 5c, d, the stir zone (SZ) area has been characterized with finer grains and the SiC particles have been uniformly distributed leading to a rise in the mechanical properties.

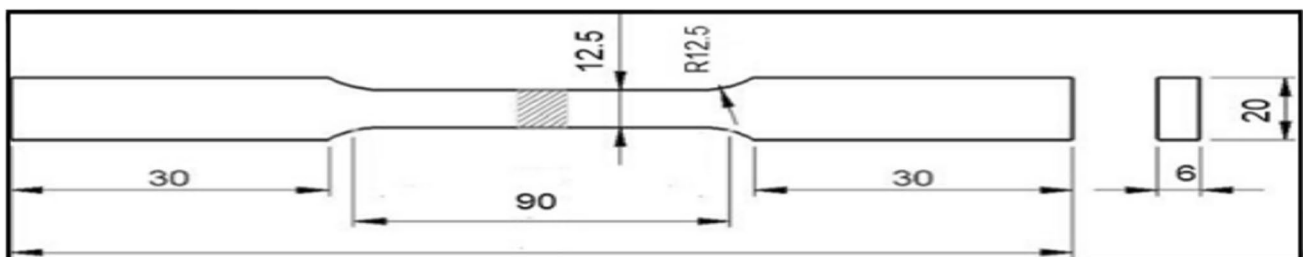


Fig. 2 The dimension of tensile specimens

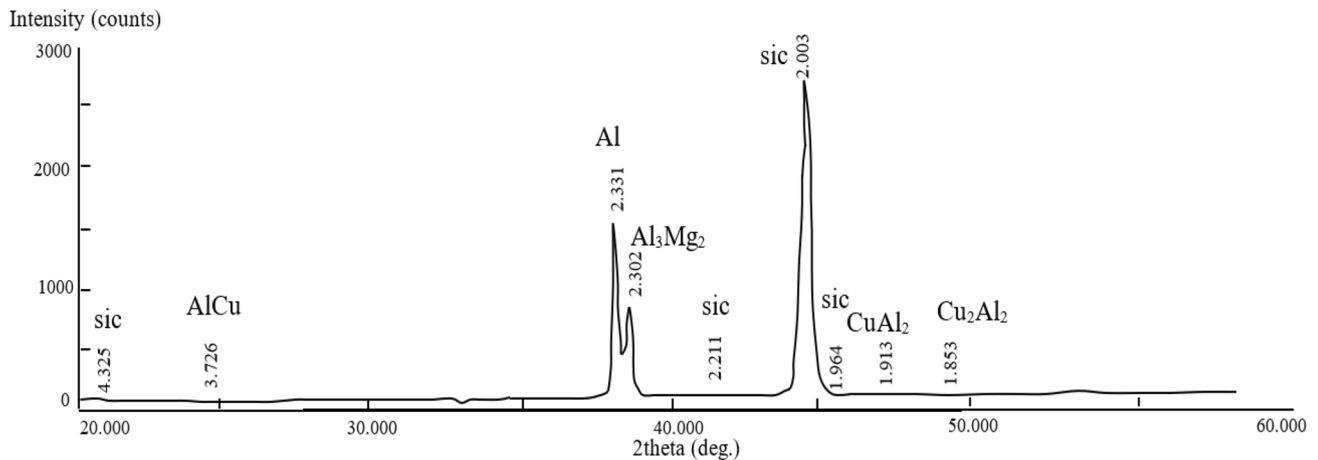


Fig. 3 X-ray pattern of FSW joints with reinforcement of 4.6% SiC

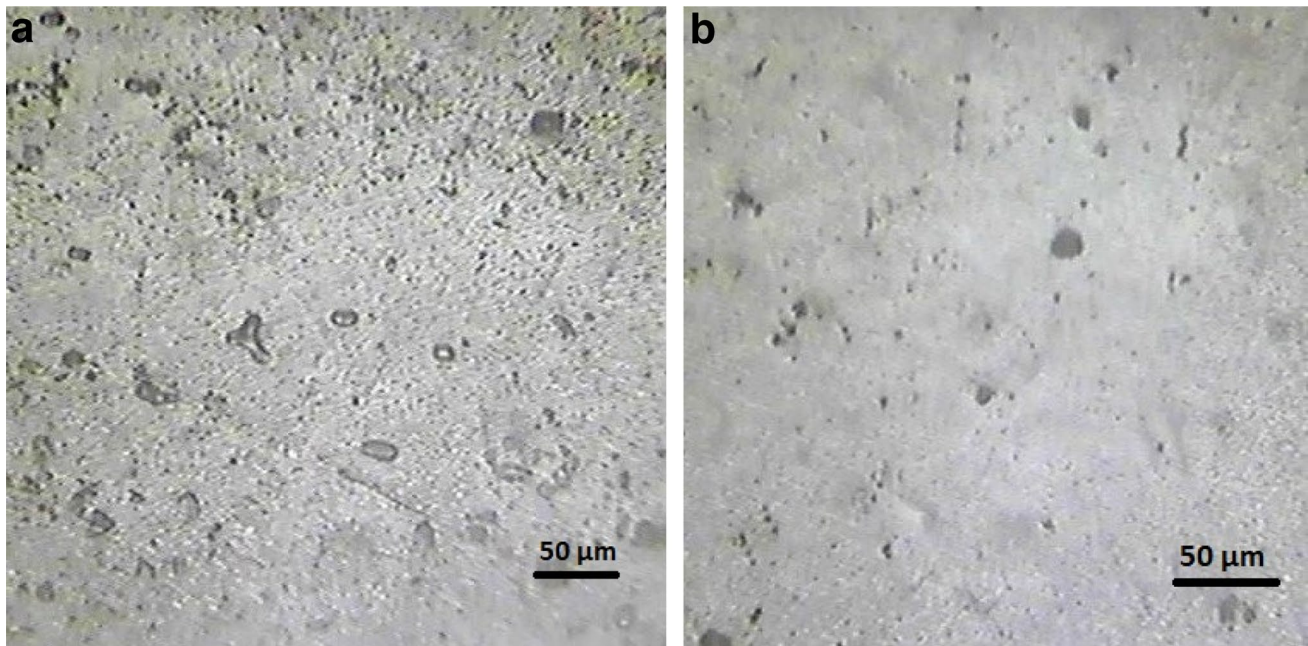


Fig. 4 The microstructures of welding alloys (a) AA2024 and (b) AA6061

Linardi et al. [14] pointed out that the alloy phases of Mg_2Si have been more concentrated in the TMAZ area. Also, Sun et al. [23] mentioned that the alloy phases of Al_2Cu are more concentrated in this zone. On the other hand, Figs. 6 and 7 show that the silicon carbide granules are denser in the EDS tests area. It has been observed from the EDS test that the Al-rich and Mg-rich phases have been found in the TMAZ area, whereas the particles of SiC have been concentrated at the SZ area.

The scanning electron microscopy microstructure of FSW of AA2024–AA6061 at the SZ area is shown in Fig. 8 for various reinforcement ratios of SiC. The results in Fig. 8a, b

show that the rise in the amount of silicon carbide granules leads to the large density of the material in the SW area. It has been also found that the microstructure is more intensive with an increase in the reinforcement ratio of SiC from 6.9 to 9.2% as shown in Fig. 8b–f. The grains size in TMAZ and SZ areas with adding SiC particles is finer as compared with that obtained without adding particles of SiC. Singh et al. [21] have attributed this issue by that the particles of SiC restrict the dynamic recovery.

The results show that the structure of the grain at the nugget area is finer granular with adding SiC particles as compared with that obtained without adding SiC particles

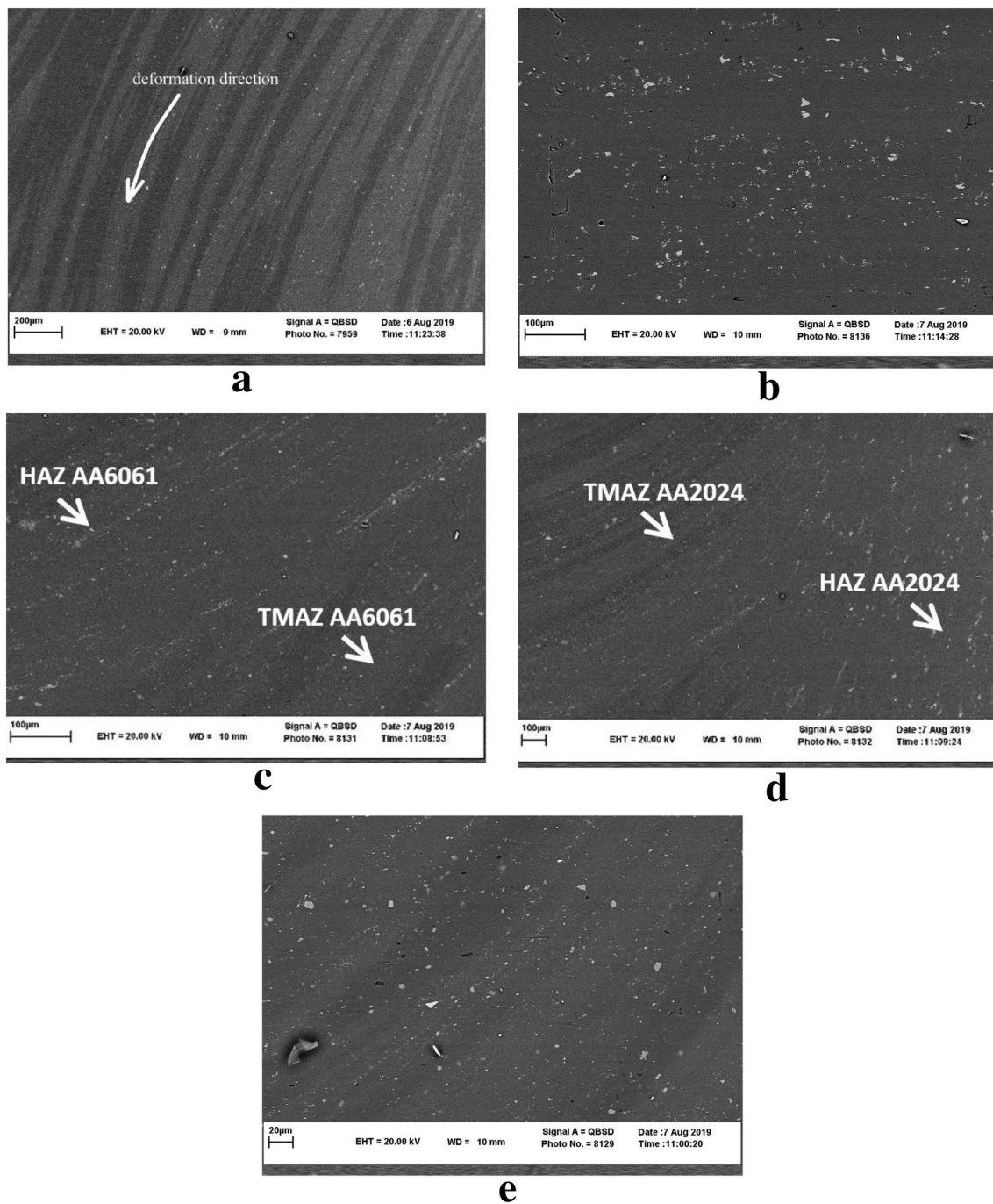


Fig. 5 The microstructures of FSW of AA2024–AA6061 for 6.9% SiC at **(a)** (TMAZ, AA6061), **(b)** SZ, **(c)** (TMAZ, AA6061 and SZ), **(d)** (TMAZ, AA2024 and SZ) and **(e)** (TMAZ, AA2024)

and with the base metals. In a practical situation, the material is under severe plastic deformation (SPD) at the SZ area, and hence, this case creates the fine grains with high-angle boundaries and it can be seen that the new grains are created in many locations at SZ area. On the other hand, the particle-stimulated nucleation (PSN) may have occurred with aluminium-based through the FSW process. Nevertheless,

the dynamic recrystallization based on PSN is possible when the dislocations start to accumulate at the strengthened particles through plastic deformation. Thus, the cause behind the finer size of grain at the NZ zone is related to the attendance of SiC particles, and hence, this considerably influences the grains size at the NZ zone. This also acts as an obstacle to the grain boundaries motion and obstructs the grain growth

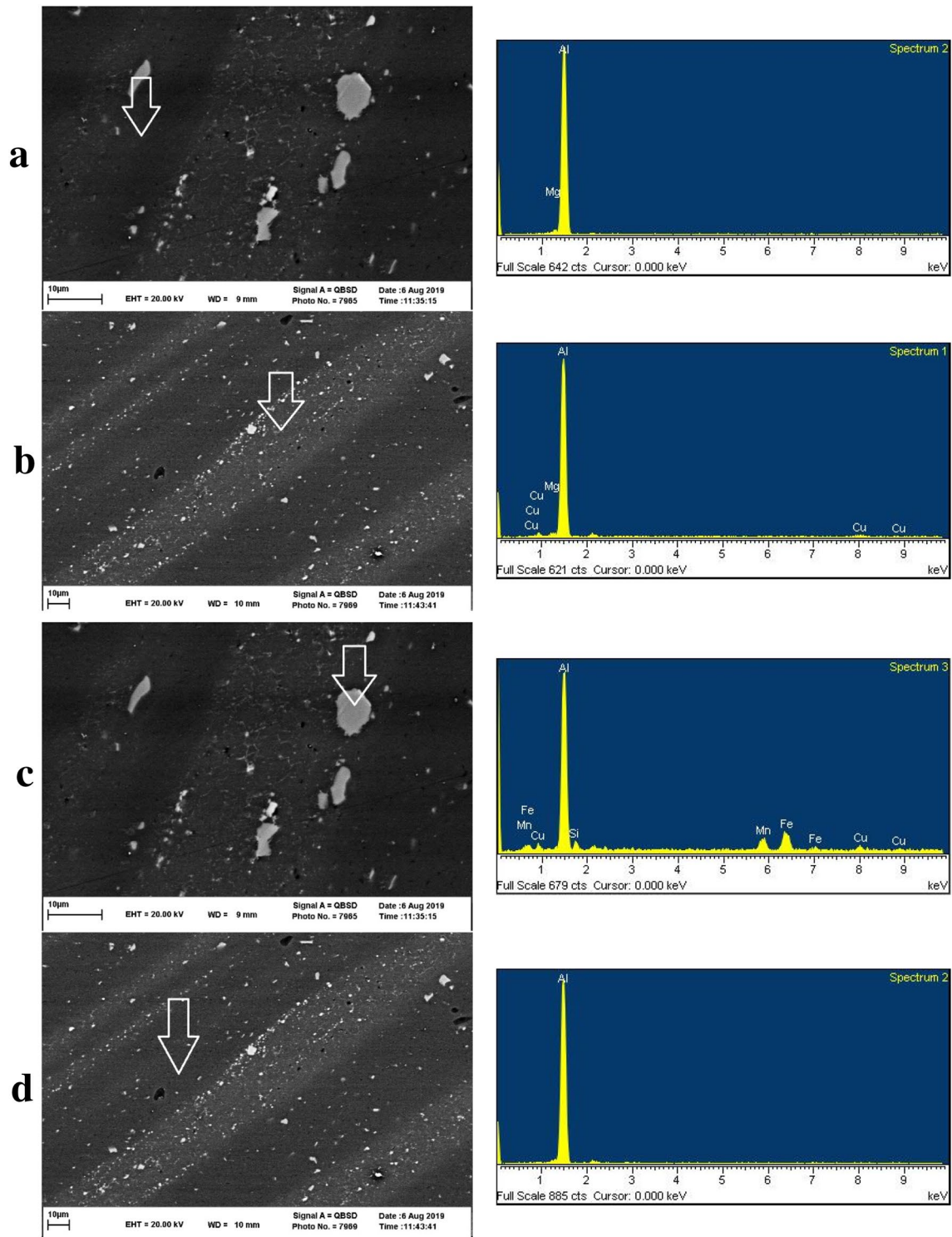


Fig. 6 The scanning electron microscopy microstructures and EDS spectrum of FSW joint of AA2024–AA6061 for (a), (c) (TMAZ, AA2024) and (b), (d) (TMAZ, AA6061)

through a Zener-pinning mechanism. Consequently, it influences the spreading of the small particles at the migration of low- and high-angle grain boundaries by using pinning pressure that reverses the driving force which is pushing the

grain boundaries [2]. Also, Sethi et al. [20] have given a similar explanation of such a case. Also, it consists of primary phase α -Al and eutectic mixture of Al, Mg and Si, where the eutectic phase contains Si and Mg. The coarse size and

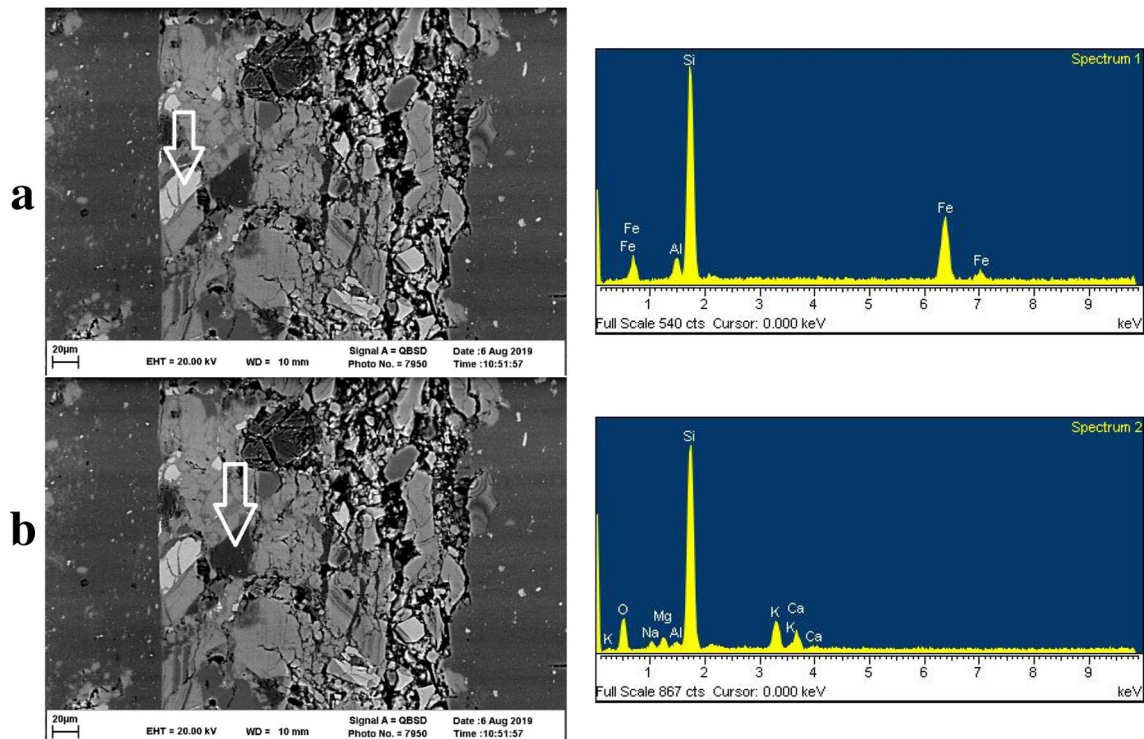


Fig. 7 The scanning electron microscopy micrograph of FSW of AA2024–AA6061 at the SZ area for 9.2% SiC

the second phase particles form a network-like distribution along the grain boundaries and inside the grain [26].

Hardness

The variations of microhardness of the FSW samples are shown in Fig. 9 for various reinforcement ratios of SiC. It is observed that the rise in the ratio of reinforcement of SiC leads to an increase in the hardness values, especially in the SZ area.

Tensile Results

The impact of adding SiC particles on the tensile properties is presented in Figs. 10 and 11. It can be demonstrated from the figures that the tensile strength is enhanced with an increase in the ratio of reinforcement of SiC up to 6.9% and decreases with a further increase in this ratio to 9.2%. The higher values of tensile strength have been obtained due to the good bonding strength between the aluminium matrix and the particles of SiC. Elnabi et al. [9] pointed out that the heat generated at the SZ area is greater than the TMAZ area. Thus, it has been found that the increase in the heat at the SZ area which has a high density of SiC leads to an increase in the tensile properties of (UTS) up to 6.9% SiC resulting from increasing the bonding of SiC particles within Al-matrix. Liu et al. [13] mentioned that the further increase

in the percentage amount of SiC leads to an increase in the formation of fine grains.

Based on the values of tensile properties of FSW samples that calculated, the largest ultimate tensile strength (UTS) has been obtained. Ande et al. [3] have attributed this issue owing to an increase in the grain refinement by adding the particles of SiC at the nugget zone compared to other samples and basic materials. Gadakh and Adepu [10] pointed out that the density of the grain boundaries increases according to the grain refinement. However, the particles of SiC partially improve the yield strength of FSW samples due to the slightly small grain size. The embedding particles of SiC have been enhanced the microhardness of FSW samples. This improvement can be accredited to the grain refinement and the distribution of fragmented and large particles of SiC at the SZ area. Furthermore, the increase in the reinforcement ratio of SiC to 9.2% creates clusters of these particles with a large size, and hence, it has a negative influence on the tensile properties.

Conclusions

The present article involves an experimental study on the improvement of the mechanical properties and microstructure of welding joints through directly adding SiC particles into a zone of friction stir welding (FSW) to

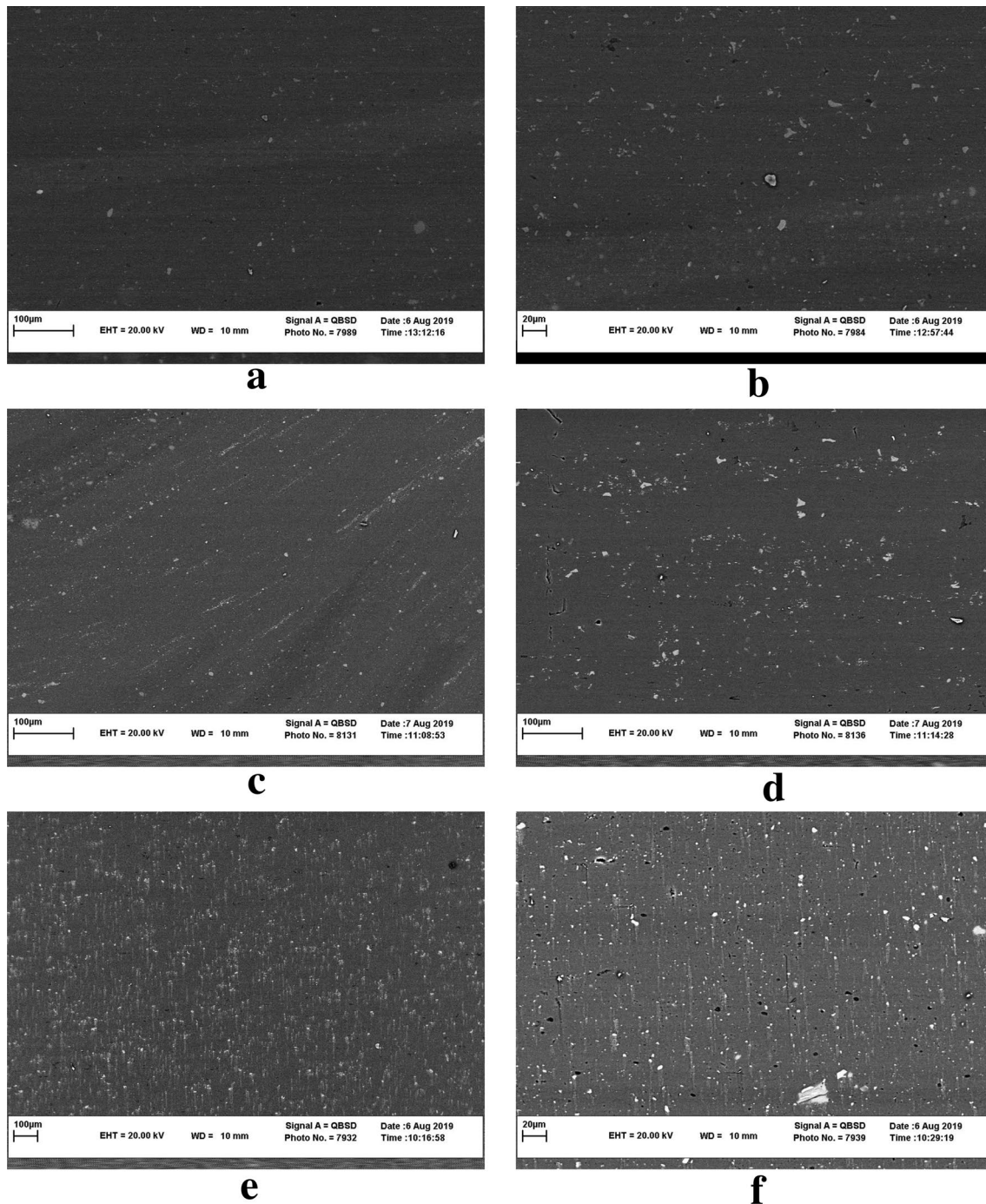


Fig. 8 The scanning electron microscopy microstructures of FSW of AA2024–AA6061 at SZ are for (a) 4.6% SiC, (b) 4.6% SiC, (c) 6.9%SiC, (d) 6.9%SiC, (e) 9.2%SiC and (f) 9.2%SiC

produce (AA6061–AA2024) SiC composites material. The FSW process has been carried out when the rotation of welding and speed has been selected to be 1040 rpm and 30 mm/min, respectively. The welding tools used during the experiments have been made from stainless steel (T31501, O1). The optical microscope, scanning

electron microscope, X-ray diffraction and EDS have been employed to investigate the microstructure characteristics and phases definition. The microhardness of FSW joints and UTS has been also measured. From this study, the following conclusions are observed:

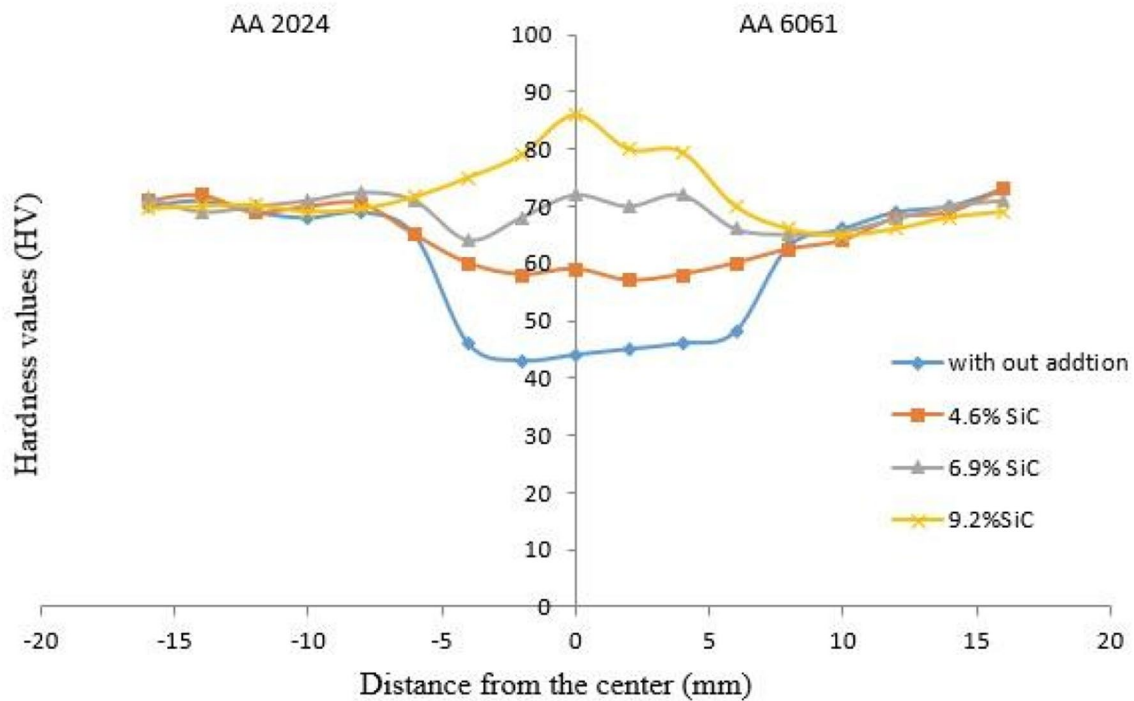


Fig. 9 Variations of microhardness of the FSW samples for various ratios of SiC

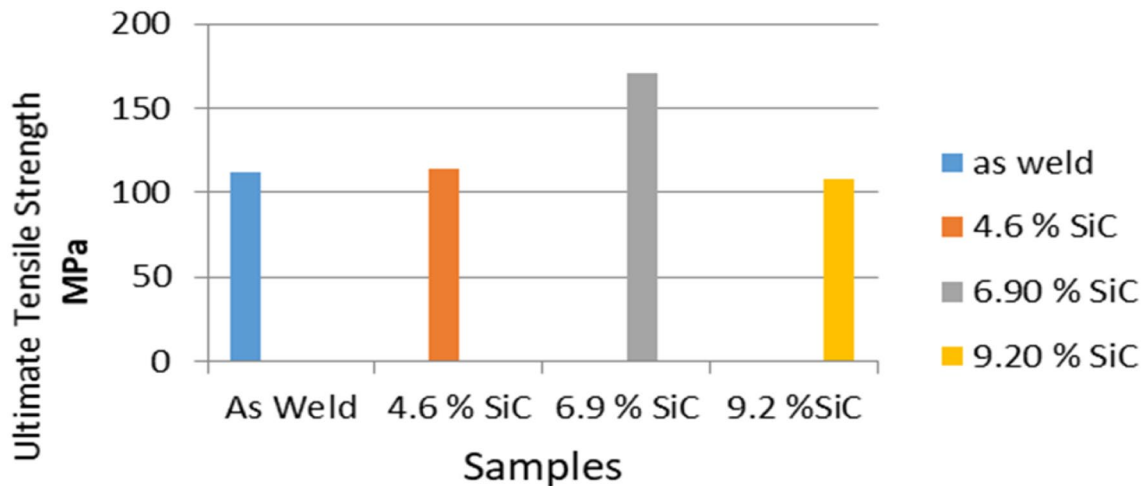


Fig. 10 Variations of UTS with adding of SiC

1. The results show that the grains in TMAZ have a coarse size and a longitudinal shape towards the deformation direction, whereas the grains in SZ have finer size.
2. The results indicate that although the SiC particles have been distributed in the deformation lines at the TMAZ area, they are in the form of clusters and characterized by a gradual size. On the other hand, the SZ area has been characterized by finer grains and the SiC particles have been uniformly distributed.
3. The grains size in TMAZ and SZ has been found finer with adding of the particles of SiC as compared to that obtained without adding SiC because the particles of SiC restrict the dynamic recovery.
4. The results indicate that the hardness values has been increased in the SZ zone with increasing in the amount of SiC particles.
5. Finally, this study demonstrates that the tensile strength increases when the reinforcement ratio of SiC is

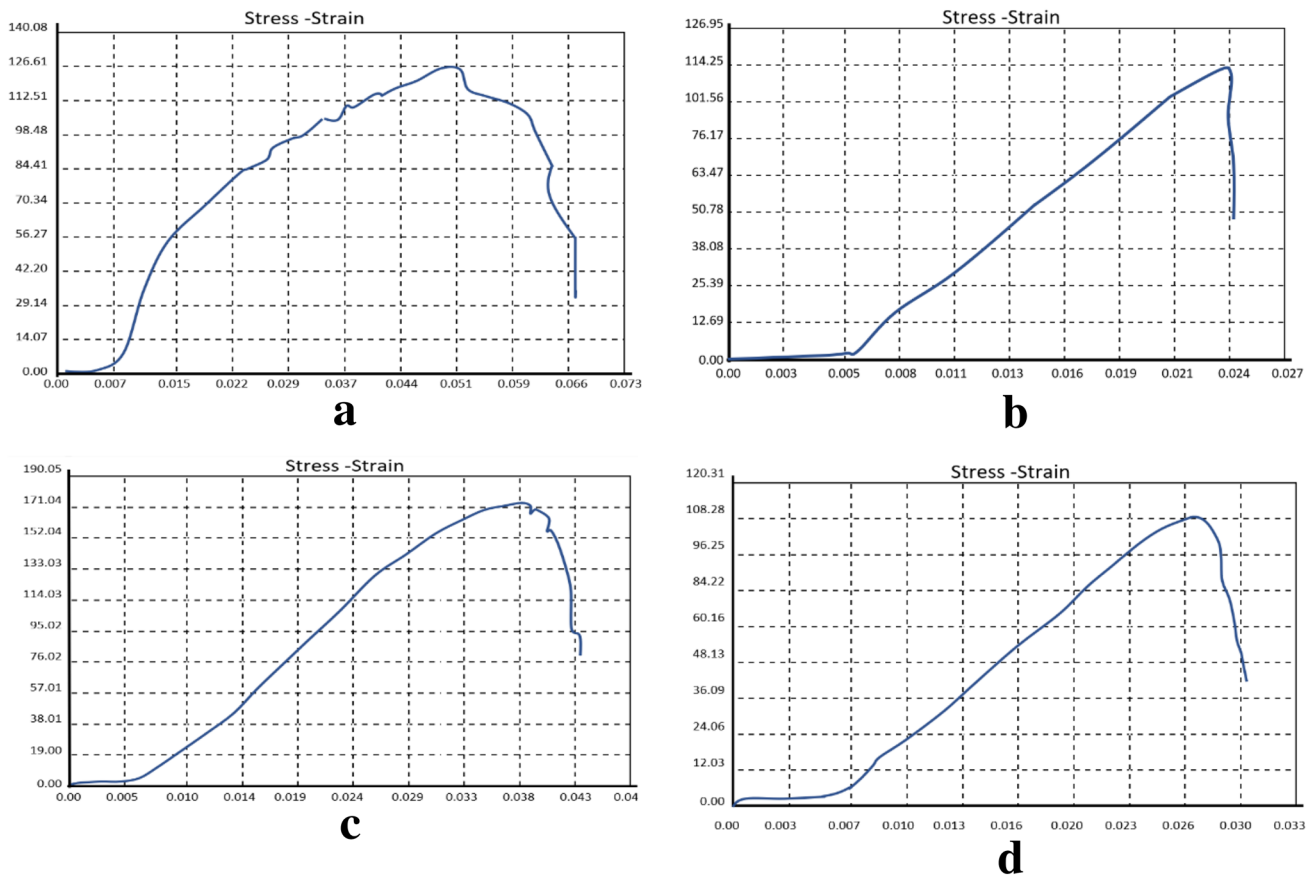


Fig. 11 Stress–strain curves of the FSW samples (a) without adding SiC, (b) 4.6% SiC, (c) 6.9% SiC and (d) 9.2% SiC

increased up to 6.9% and decreases with further increasing of this ratio which up to 9.2%. It evident that the reinforcement ratio of SiC particles plays a significant role for obtaining a best thermomechanical properties of the composite material. Therefore, this issue required a careful consideration to reach a desired objective.

Acknowledgements We would like to thank the Middle Technical University, Baghdad, Iraq, and the Northern Technical University, Mosul, Iraq, for their laboratory provision for this work.

Data Availability Statement The raw/processed data required to reproduce these findings cannot be shared at this time as the data also form part of an ongoing study.

References

- U. Acharya, B.S. Roy, S.C. Saha, Effect of tool rotational speed on the particle distribution in friction stir welding of AA6092/17.5 SiCp-T6 composite plates and its consequences on the mechanical property of the joint. *Defence Technol.* (2019). <https://doi.org/10.1016/j.dt.2019.08.017>
- H. Ali, G.Y. Guney, High temperature characteristics of Al2024/SiC metal matrix composite fabricated by friction stir processing. *Mater. Sci. Eng. A.* **731**, 487–494 (2018)
- R. Ande, G. Piyush, K. Dinesh, D. Hitesh, Microstructural and wear characteristics of friction stir processed Al-7075/SiC reinforced aluminium composite. *Mater. Today Proc.* **18**, 4092–4101 (2019)
- G. Azimi-Roeeen, S.F. Kashani-Bozorg, M. Nosko, L. Orovciik, S. Lotfian, Effect of multi-pass friction stir processing on textural evolution and grain boundary structure of Al-Fe₃O₄ system. *J. Market. Res.* **9**(1), 1070–1086 (2020)
- C. Boonchouytan, B. Rawangwong, Effect of heat treatment T6 on the friction stir welded SSM 6061 aluminum alloys. *Energy Proc.* **56**, 172–180 (2014)
- D. Deepak, R.S. Sidhu, V. Gupta, Preparation of 5083 Al-SiC surface composite by friction stir processing and its mechanical characterization. *Int. J. Mech. Eng.* **3**(1), 1–11 (2013)
- I. Dinaharan, Influence of ceramic particulate type on microstructure and tensile strength of aluminium matrix composites produced using friction stir processing. *J. Asian Ceramic Soc.* **4**(2), 209–218 (2016)
- G. Elatharasan, V.S. Kumar, An experimental analysis and optimization of process parameter on friction stir welding of AA6061-T6 aluminium alloy using RSM. *Proc. Eng.* **64**, 1227–1234 (2013)
- M.M.A. Elnabi, A.B. Elshalakany, M.M. Abdel-Mottaleb, T.A. Osman, A.E. Mokadem, Influence of friction stir welding parameters on metallurgical and mechanical properties of

- dissimilar AA5454–AA7075 aluminium alloys. *J. Market. Res.* **8**(2), 1684–1693 (2019)
10. V.S. Gadakh, K. Adepu, Heat generation model for taper cylindrical pin profile in FSW. *J. Market. Res.* **2**(4), 370–375 (2013)
 11. N. Gangil, S. Maheshwarib, A.N. Siddiqueec, M.H. Abidid, M.A. El-Meligyd, J.A. Mohammede, Investigation on friction stir welding of hybrid composites fabricated on Al–Zn–Mg–Cu alloy through friction stir processing. *J. Market. Res.* **8**(5), 3733–3740 (2019)
 12. Ö. Güler, N. Bağc, A short review on mechanical properties of graphene reinforced metal matrix composites. *J. Market. Res.* (2020). <https://doi.org/10.1016/j.jmrt.2020.01.077>
 13. N. HuijieLiu, H. Yanying, Z. Yunqiang, Microstructural characteristics and formation mechanism of friction stir welds of SiC particulates reinforced Al–Si matrix composites. *Mater. Lett.* **158**, 136–139 (2015)
 14. E. Linardi, R. Haddad, L. Lanzani, Stability analysis of the Mg₂Si phase in AA6061 aluminium alloy. *Proc. Mater. Sci.* **1**, 550–557 (2012)
 15. R.S. Mishra, Z. Ma, Friction stir welding and processing. *Mater. Sci. Eng.* **50**(1), 1–78 (2005)
 16. M.A. Pasha, P.R. Reddy, P. Laxminarayana, I.A. Khan, The effects of SiC particle addition as reinforcement in the weld zone during friction stir welding of magnesium alloy AZ31B. *IRA-Int. J. Technol. Eng.* **3**(3), 154–163 (2016)
 17. N. Pol, G. Verma, R.P. Pandey, T. Shanmugasundaram, Fabrication of AA7005/TiB₂-B₄C surface composite by friction stir processing: evaluation of ballistic behaviour. *Defence Technol.* **15**(3), 363–368 (2019)
 18. P. Prakash, S.K. Jha, S.P. Lal, A study of process parameters on friction stir welded AA6061 aluminium alloy. *Int. J. Innov. Res. Sci. Eng. Technol.* **2**(6), 2319–8753 (2013)
 19. S. Rathee, S. Maheshwari, A.N. Siddiquee, M. Srivastava, Effect of tool plunge depth on reinforcement particles distribution in surface composite fabrication via friction stir processing. *Defence Technol.* **13**(2), 86–91 (2017)
 20. D. Sethi, U. Acharya, T. Medhi, S. Shekhar, B.S. Roy, Microstructural and mechanical property of friction stir welded Al7075/TiB₂ aluminium matrix composite. *Mater. Today Proc.* (2020). <https://doi.org/10.1016/j.matpr.2020.01.198>
 21. T. Singh, S. Tiwari, D. Shukla, Friction-stir welding of AA6061-T6: the effects of Al₂O₃ nano-particles addition. *Res. Mater.* **1**, 100005 (2019)
 22. Y. Sun, H. Fujii, The effect of SiC particles on the microstructure and mechanical properties of friction stir welded pure copper joints. *Mater. Sci. Eng.* **528**(16–17), 5470–5475 (2011)
 23. S. Sun, Y. Fang, L. Zhang, C. Li, S. Hu, Effects of aging treatment and peripheral coarse grain on the exfoliation corrosion behaviour of 2024 aluminium alloy using SR-CT. *J. Market. Res.* (2020). <https://doi.org/10.1016/j.jmrt.2020.01.069>
 24. A. Thangarasu, N. Nurugan, I. Dinaharan, S.J. Vijay, Influence of traverse speed on microstructure and mechanical properties of AA6082-TiC surface composite fabricated by friction stir processing. *Proc. Mater. Sci.* **5**, 2115–2121 (2014)
 25. N. Yuvaraj, S. Aravindan, Fabrication of Al5083/B₄C surface composite by friction stir processing and its tribological characterization. *J. Market. Res.* **4**(4), 398–410 (2015)
 26. C. Zhang, G. Huang, D. Zhang, Z. Sun, Q. Liu, Microstructure and mechanical properties in dissimilar friction stir welded AA2024/7075 joints at high heat input: effect of post-weld heat treatment. *J. Mater. Res. Technol.* **9**(6), 14771–14782 (2020)
 27. L. Zhang, G. Shi, X. Kun, H. Wu, Q. Li, J. Wu, Z. Wang, Phase transformation and mechanical properties of B₄C/Al composites. *J. Market. Res.* (2019). <https://doi.org/10.1016/j.jmrt.2019.12.042>
 28. Y. Zhao, X. Kai, G. Chen, W. Lin, C. Wang, Effects of friction stir processing on the microstructure and super plasticity of in situ nano-ZrB₂/2024Al composite. *Progr. Nat. Sci. Mater. Int.* **26**(1), 69–77 (2016)

Publisher's Note Springer Nature remains neutral with regard to jurisdictional claims in published maps and institutional affiliations.